SYSTEM SIZE AND BEAM ENERGY DEPENDENCE OF HADRONIC PRODUCTION AND FREEZE-OUT*

Orpheus I. Mall

for the STAR Collaboration

University of California, Davis, One Shields Ave. Davis, CA 95616, USA

(Received December 6, 2011)

We present results from STAR for Au + Au 19.6 GeV and Cu + Cu 22.4 GeV collisions from previous RHIC runs. Particle spectra for $\pi^{\pm}$, $K^{\pm}$, p and $\bar{p}$ are studied as a function of $m_{\mathrm{T}} - m_0$. We report on the K/π and p/π ratios from these collisions. Freeze-out parameters from both chemical freeze-out and kinetic freeze-out are extracted from the spectra. We make systematic comparisons with the data from 7.7, 11.5 and 39 GeV Au + Au collisions taken in 2010 during the RHIC Beam Energy Scan.

DOI:10.5506/APhysPolBSupp.5.491
PACS numbers: 25.75.Nq, 25.75.–q, 25.75.Dw, 12.38.Mh

1. Introduction

In the search for the critical point and the onset of deconfinement, RHIC has conducted a Beam Energy Scan by colliding Au + Au at a range of energies from 7.7 to 62.4 GeV. The STAR detector provides excellent particle identification extended to a large range in p_{T} by the addition of the Time-of-Flight system. Mid-rapidity charged hadron spectra are utilized to study the freeze-out dynamics of the matter created in these collisions.

Lattice calculations with non-zero quark masses and finite strange quark mass, point to a crossover for QCD matter at vanishing baryon chemical potential ($\mu_B = 0$) [1, 2]. Lattice calculations at finite μ_B allow for a first order phase transition at high μ_B ending at a critical point approaching lower μ_B [3]. Variation of the initial energy density and the net baryon density allow handles on the freeze-out temperature and the baryon chemical potential. Experimentally, this can be achieved by variation of the collision energy and heavy-ion species.

* Presented at the Conference “Strangeness in Quark Matter 2011”, Kraków, Poland, September 18–24, 2011.

The experimental effort to map the QCD phase boundary focuses on the search for the onset of deconfinement, the first order phase transition, and the critical point. Experimental programs have been conducted to this end at the SIS, AGS, SPS, RHIC and LHC and combined with the RHIC Beam Energy Scan cover a wide range of the chemical freeze-out curve. The RHIC Beam Energy Scan has extended coverage at intermediate μ_B with Au + Au collisions at energies from $\sqrt{s_{NN}}$=7.7 to 62.4 GeV and the STAR detector has collected unprecedented statistics at these energies [4]. Based on findings from NA49 of $p+p$, C + C, and Si + Si collisions, the NA61 SHINE experiment proposes to conduct a system size scan. RHIC has collided Cu nuclei at $\sqrt{s_{NN}}$=22.4, 62.4 and 200 GeV with STAR recording 1 M, 10 M, and 24 M events respectively [5]. The Cu + Cu system is the optimal size for study of system size dependence of freeze-out dynamics. It is not so small that QGP is not expected to be formed, and not so large that comparisons with Au + Au are difficult.

2. Results and discussion

Cu + Cu 22.4 GeV and Au + Au 19.6 GeV collisions from years 2005 and 2001 are studied with approximately 1 M and 45 K events respectively. We compare central collisions of Cu + Cu 22.4 GeV to central collisions of Au + Au 19.6 GeV and to peripheral collisions of Au + Au 19.6 GeV of similar size $\langle N_{\mathrm{part}}\rangle$. The Monte Carlo Glauber model is used to simulate the collisions and fit the raw charged multiplicity via a negative binomial distribution to determine centrality cuts. The Glauber model shows greater transverse overlap area for central Cu + Cu collisions *vs.* peripheral Au + Au collisions of similar size. From model calculations, collisions of Cu + Cu 22.4 GeV 0–5% central have an $\langle N_{\mathrm{part}}\rangle = 108$ while Au + Au 19.6 GeV 30–50% collisions have an $\langle N_{\mathrm{part}}\rangle = 95$.

2.1. Charged hadron $m_{\mathrm{T}}-m_0$ spectra

Charged hadron $m_{\mathrm{T}}-m_0$ ($m_{\mathrm{T}}^2 = p_{\mathrm{T}}^2+m_0^2$, m_0 is the hadron mass) spectra were studied for $\pi^{\pm}$, $K^{\pm}$, p and $\bar{p}$. Particle identification is accomplished via ionization due to energy loss in the STAR TPC [6]. Raw spectra are corrected for detector acceptance, reconstruction efficiency, and energy loss prior to entering the detector, accomplished via embedding of Monte Carlo tracks in the data passed through the reconstruction chain. Proton spectra have been corrected for background kick-out protons. Corrections not included are weak decay contributions to the pion spectra and feed-down contributions to the proton spectra. The spectra are shown in Fig. 1.

The spectra for Au + Au 19.6 GeV and Cu + Cu 22.4 GeV GeV are similar with three features of interest. Spectra for Cu + Cu 0–5% central collisions lie between Au + Au 10–30% and 30–50% as may be expected from N_{part}

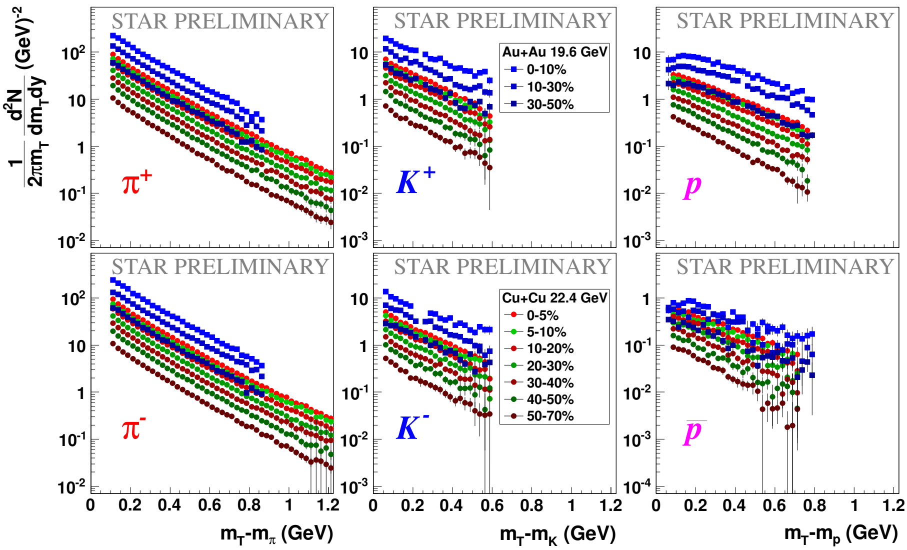

Fig. 1. Invariant yields of $\pi^{\pm}$, $K^{\pm}$, p and $\bar{p}$ from Cu + Cu 22.4 GeV and Au + Au 19.6 GeV collisions for various centralities as a function of transverse kinetic energy. Errors are statistical+systematic for Cu + Cu 22.4 GeV and statistical for Au + Au 19.6 GeV.

scaling. Central Cu + Cu p yields are closer to Au + Au 30–50% while the $\bar{p}$ yields for central Cu + Cu are closer to Au + Au 10–30% collisions. Lastly, there is a turnover at low $m_{\rm T}-m_0$ for p spectra of Au + Au collisions which is not observed in Cu + Cu at this energy. All particle spectra are fit with several models including Bose–Einstein/Fermi–Dirac, Maxwell–Boltzmann, $m_{\rm T}$-exp, $p_{\rm T}$-exp, $p_{\rm T}^2$-exp, and blast-wave models. These fits were used to extrapolate the total integrated invariant yields and study systematic errors. Fits to π spectra yield lowest χ^2 with Bose–Einstein fits. K mesons were well fit by either Bose–Einstein, m_T-exp, $p_{\rm T}$-exp, or Maxwell–Boltzmann. Protons were best fit by blast wave.

2.2. Net-baryon density and strangeness

The mid-rapidity yields are used to study comparative hadronic production utilizing particle ratios in comparison with STAR data of Au + Au and Cu + Cu collisions at 62.4, 130 and 200 GeV (Fig. 2 upper and middle-left panels) [5, 7] (all errors: $\sigma^2 = \sigma^2_{\rm stat} + \sigma^2_{\rm sys}$). The p/π^+ ratio decreases with increasing $\sqrt{s_{NN}}$ and increases with centrality. The $\bar{p}/\pi^-$ ratio increases with increasing beam energy and shows no dependence on centrality. The imbalance of baryon to anti-baryon production can be seen via the imbalance of p/π^+ and $\bar{p}/\pi^-$ which increases at lower beam energies. The effect seems less pronounced in smaller systems at low energy. Net-baryon density $(dN/dy)_{p-\bar{p}}/(\langle N_{\rm part}\rangle/2)$ increases with centrality and with decreasing beam energy (Fig. 2 lower-left panel).

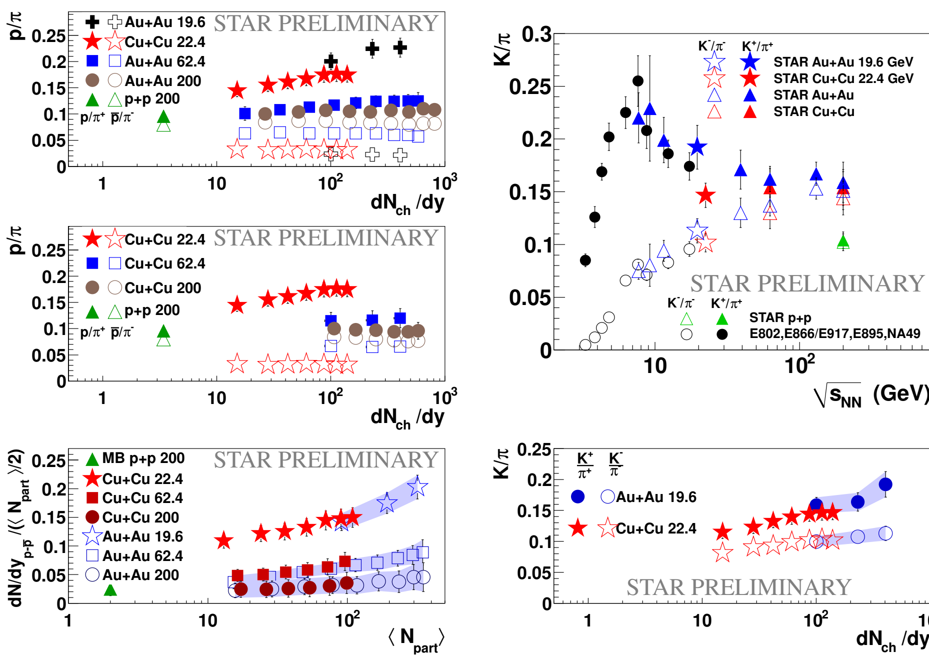

Fig. 2. Upper-left: The p/π^+ and $\bar{p}/\pi^-$ ratios *vs.* multiplicity for Cu + Cu 22.4 GeV compared to Au + Au and (middle-left) Cu + Cu systems. Lower-left: Net-baryon density *vs.* $\langle N_{\rm part}\rangle$ for Cu + Cu and Au + Au systems with STAR [7, 5]. Upper-right: K/π ratio *vs.* $\sqrt{s_{NN}}$ for the SIS, AGS, SPS and STAR data including the Beam Energy Scan [8, 9, 10, 11, 12, 13, 14, 15]. Lower-right: K/π ratio *vs.* centrality for Cu + Cu 22.4 GeV and Au + Au 19.6 GeV systems.

Strangeness production may be studied via K/π ratios. At high energies, the K^+/π^+ ratio is lower for the Cu + Cu system in comparison with the Au + Au system but consistent within errors (Fig. 2 upper and lower right panels) [5, 7]. At lower energies, as the difference between the K^+/π^+ and K^-/π^- ratios increases, we find the Cu + Cu 22.4 GeV 0–5% central system has lower K^+/π^+ ratio than Au + Au 19.6 GeV 0–10% central collisions ($< 1.5\sigma$ difference for $\sigma^2 = \sigma^2_{\rm stat} + \sigma^2_{\rm sys}$). For collisions of similar $\langle N_{\rm part}\rangle$ the K^+/π^+ ratio is consistent within errors, though the Cu + Cu 22.4 GeV ratios appear to be lower than Au + Au 19.6 GeV.

2.3. Kinetic and chemical freeze-out

Spectra from Cu + Cu 22.4 GeV collisions were fit with a blast-wave model [16] to study kinetic freeze-out which shows higher $T_{\rm kin}$ and lower $\langle\beta_{\rm T}\rangle$ than Au + Au 19.6 GeV collisions of similar size. Furthermore, Cu + Cu systems appear to have higher kinetic freeze-out temperatures than Au + Au for central collisions at similar energies [5, 7, 16]. Systematic errors are predominantly correlated and arise mainly from the low $p_{\rm T}$ cut of the π spectra where the behavior is dominated by Bose–Einstein statistics.

A statistical model was fit to the mid-rapidity particle ratios in order to extract the chemical freeze-out temperature $T_{\rm ch}$, quark chemical potential μ_q, strange quark chemical potential μ_s, and the strangeness saturation factor γ_s [19, 20]. The baryon chemical potential is given by $\mu_B = 3\mu_q$. At RHIC energies, the chemical freeze-out temperature is found to be consistent within errors across centralities, energies and system sizes [7, 5]. The freeze-out temperature for Cu + Cu 22.4 GeV 0–5% central collisions at $T_{\rm ch} = 160.3 \pm 5.4$ MeV is consistent with that of Au + Au 19.6 GeV 0–10% central collisions at $T_{\rm ch} = 157.2 \pm 8.3$ MeV (Fig. 3, left panel). The extracted baryon chemical potential differs, found to be $\mu_B = 138.9 \pm 8.4$ MeV for Cu + Cu 22.4 GeV 0–5% central and $\mu_B = 187.0 \pm 19.4$ MeV for Au + Au 19.6 GeV 0–10% central collisions. The difference in μ_B is less than 2σ (all errors: $\sigma^2 = \sigma^2_{\rm stat} + \sigma^2_{\rm sys}$).

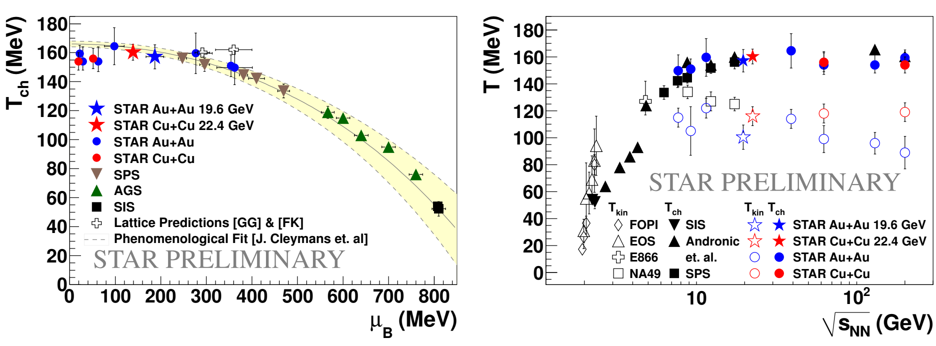

Fig. 3. Left: Chemical freeze-out model fits to particle ratios for SIS, AGS, SPS and STAR data showing $T_{\rm ch}$ *vs.* μ_B for the most central collisions. Right: Freeze-out dynamics showing $T_{\rm ch}$ and $T_{\rm kin}$ *vs.* $\sqrt{s_{NN}}$. STAR results are from mid-rapidity yields whereas SIS, AGS, and SPS are 4π yields [3,5,7,8,9,10,11,12,13,17,14,15,18].

Collision evolution may be studied via comparison of the chemical freeze-out and kinetic freeze-out studies. The separation between the $T_{\rm ch}$ and $T_{\rm kin}$ is found to increase with collision energy (Fig. 3, right panel). It is possible that the effect is less pronounced for Cu + Cu systems as they tend to have systematically higher $T_{\rm kin}$ in comparison with Au + Au systems of similar beam energies. This may have interesting implications for the time evolution $(\tau_{\rm kin} - \tau_{\rm ch})$ of the system.

Study of the Cu + Cu system provides vital information about the matter created in heavy-ion collisions and its properties. Cu + Cu systems do not necessarily follow simple $N_{\rm part}$ scaling and may be used to decouple initial energy density and initial baryon density effects. The NA61 SHINE proposal expects smaller system sizes will lead to higher chemical freeze-out temperatures and may help to leverage freeze-out towards a first-order phase transition and/or critical point [21]. This was not a significant effect in our data. The more notable effect was on the baryon chemical potential indicating that perhaps heavier ions are the key. A complication for heavier ions arises from non-spherical geometries, for example $^{238}_{92}$U with a $\beta_2 = 0.215$ [22]. The increased transverse energy density of head-on U + U collisions is desirable, but the cross-section is low. It will be challenging to resolve head-on collisions from other orientations.

REFERENCES

[1] Y. Aoki *et al.*, *Nature* **443**, 675 (2006).
[2] M. Cheng *et al.*, *Phys. Rev.* **D77**, 014511 (2008).
[3] R.V. Gavai *et al.*, *Phys. Rev.* **D78**, 114503 (2008).
[4] M.M. Aggarwal *et al.*, `arXiv:1007.2613 [nucl-ex]`.
[5] M.M. Aggarwal *et al.*, *Phys. Rev.* **C83**, 034910 (2011).
[6] M. Anderson *et al.*, *Nucl. Instum. Methods* **A499**, 659 (2003).
[7] B.I. Abelev *et al.*, *Phys. Rev.* **C79**, 034909 (2009).
[8] J. Cleymans *et al.*, *J. Phys.G* **25**, 281 (1999).
[9] M.A. Lisa *et al.*, *Phys. Rev. Lett.* **75**, 2662 (1995).
[10] C. Muntz, `arXiv:nucl-ex/9806002`.
[11] J.L. Klay *et al.*, *Phys. Rev.* **C68**, 054905 (2003).
[12] S.V. Afanasiev *et al.*, *Phys. Rev.* **C66**, 054902 (2002).
[13] A. Andronic *et al.*, *Nucl. Phys.* **A772**, 167 (2006).
[14] B.I. Abelev *et al.*, *Phys. Rev.* **C81**, 024911 (2010).
[15] L. Kumar, *J. Phys.G* **38**, 124145 (2011).
[16] E. Schnedermann *et al.*, *Phys. Rev.* **C48**, 2462 (1993).
[17] W. Reisdorf *et al.*, *Nucl. Phys.* **A612**, 493 (1997).
[18] Z. Fodor, S.D. Katz, `arXiv:0908.3341 [hep-ph]`.
[19] P. Braun-Munzinger, I. Heppe, J. Stachel, *Phys. Lett.* **B465**, 15 (1999).
[20] M. Kaneta, N. Xu, `arXiv:nucl-th/0405068`.
[21] N. Antoniou *et al.*, CERN-SPSC-2006-034, 2006.
[22] P. Moller *et al.*, *Atomic Data Nucl. Data Tables* **59**, 185 (1995).